First results on double β-decay modes of Cd, Te, and Zn Isotopes

T. Bloxham,[1] A. Boston,[4] J. Dawson,[5] D. Dobos,[2] S. P. Fox,[7] M. Freer,[1] B. R. Fulton,[7] C. Gößling,[2] P. F. Harrison,[6] M. Junker,[3] H. Kiel,[2] J. McGrath,[7] B. Morgan,[6] D. Münstermann,[2] P. Nolan,[4] S. Oehl,[2] Y. Ramachers,[6] C. Reeve,[5] D. Stewart,[6] R. Wadsworth,[7] J. R. Wilson,[5] and K. Zuber[5]

[1]*School of Physics and Astronomy, University of Birmingham, B15 2TT, United Kingdom.*
[2]*Lehrstuhl für Experimentelle Physik IV, Universität Dortmund, Otto-Hahn Str. 4, D-44227 Dortmund, Germany*
[3]*Laboratori Nazionali del Gran Sasso, S.S. 17, BIS km. 18.910, 67010, Assergi, L'Aquila, Italy*
[4]*Department of Physics, University of Liverpool, Liverpool L69 7ZE, United Kingdom*
[5]*Department of Physics and Astronomy, University of Sussex, Brighton, BN1 9QH, United Kingdom*
[6]*Department of Physics, University of Warwick, Coventry CV4 7AL, United Kingdom*
[7]*Department of Physics, University of York, Heslington, York, YO10 5DD, United Kingdom*

(Received 18 October 2006; published 3 August 2007)

Four 1-cm^3 CdZnTe semiconductor detectors were operated in the Gran Sasso National Laboratory to explore the feasibility of such devices for double β-decay searches as proposed for the COBRA experiment. The research involved background studies accompanied by measurements of energy resolution performed at the surface. Energy resolutions sufficient to reduce the contribution of two-neutrino double β-decay events to a negligible level for a large-scale experiment have already been achieved and further improvements are expected. Using activity measurements of contaminants in all construction materials a background model was developed with the help of Monte Carlo simulations and major background sources were identified. A total exposure of 4.34 kg·days of underground data have been accumulated allowing a search for neutrinoless double β-decay modes of seven isotopes found in CdZnTe. Half-life limits (90% C.L.) are presented for decays to ground and excited states. Four improved lower limits have been obtained, including zero neutrino double electron capture transitions of ^{64}Zn and ^{120}Te to the ground state, which are 1.19×10^{17} years and 2.68×10^{15} years, respectively.

DOI: 10.1103/PhysRevC.76.025501 PACS number(s): 23.40.−s, 21.10.Tg, 27.60.+j, 29.40.Wk

I. INTRODUCTION

In recent years, a range of neutrino oscillation experiments [1–3] have successfully proved that neutrinos are massive particles. Although such experiments are sensitive to a mass-difference rather than absolute neutrino mass, the data suggest a neutrino mass eigenstate of at least 50 meV. To further probe the neutrino's properties, it is necessary to look to other processes such as neutrinoless double β decay ($0\nu\beta\beta$), which violates lepton number by two units; observation of this process would confirm the Majorana nature of the neutrino and the rate of this rare decay is proportional to the absolute neutrino mass scale. For recent reviews of double β decay see Refs. [4] and [5].

The COBRA experiment uses CdZnTe (CZT) semiconductors to search for $0\nu\beta\beta$ [6]. CZT contains nine double β emitters, five of which can decay via double β decay, i.e., emitting two electrons, and four of them via either double electron capture, a combination of a positron emission with electron capture or double positron emission. The study of the positron and electron capture modes can be used for lepton number-violating decay searches on an equivalent level to $0\nu\beta\beta$; however, the phase space for the positron modes is strongly reduced, making them less sensitive. Nevertheless, is has been shown that the positron/electron capture mixed modes have an enhanced sensitivity to right-handed weak currents and thus can help to disentangle the underlying physics mechanism of $0\nu\beta\beta$ if observed [7]. In addition, excited state transitions can be explored with high efficiency and low background using coincidence techniques among the detectors. These decays would allow an independent search for double β decay searching for the deexcitation photons together with the electron signal.

The main focus of the work described in this article is the study of background through measurements performed underground, and energy resolution studies carried out in a surface laboratory. Optimization of these quantities is vital for a successful search for $0\nu\beta\beta$, because, in the background limited case, the observable half-life depends on them with a square root behavior. In addition, half-life limits for seven double β isotopes contained in natural CZT have been determined from data collected with a small prototype detector accumulating an exposure of 4.34 kg·days.

II. SENSITIVITY

Although COBRA is able to search for $0\nu\beta\beta$ in a number of isotopes, the sensitivity for the modes with lower Q values will ultimately be limited by background contributions from two neutrino double β ($2\nu\beta\beta$) decays of the isotopes with higher Q values. The contribution of $2\nu\beta\beta$ decay events to the current data set is negligible, but for a very sensitive neutrino mass search, COBRA will focus on ^{116}Cd, which has the highest Q value of 2809 keV for the nuclear decay to ^{116}Pd. A peak will occur at this energy in the sum energy spectrum for the case of $0\nu\beta\beta$.

Crucial experimental parameters, in addition to the mass of the detector/sample, are energy resolution and the number of contaminating background events in this range, as shown

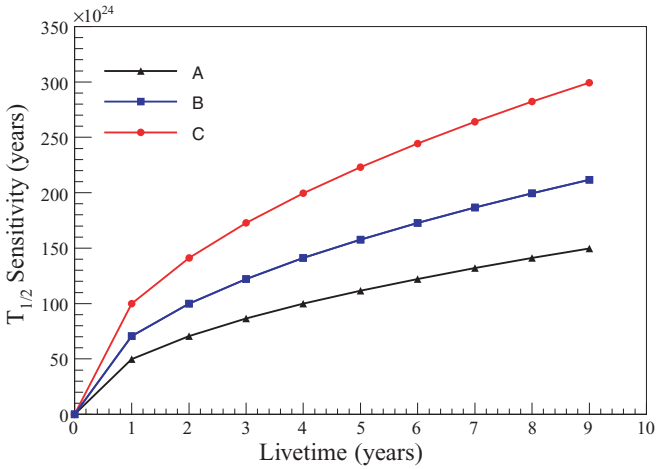

FIG. 1. (Color online) The expected half-life sensitivity for $0\nu\beta\beta$-decay of ^{116}Cd in an array of 64,000 1-cm^3 detectors, enriched to 90% in ^{116}Cd for three scenarios of background and energy resolution (ΔE = FWHM): A = 10^{-3} counts/(keV kg year), $\Delta E = 2\%$ at 2.8 MeV; B = 10^{-3} counts/(keV kg year), $\Delta E = 1\%$ at 2.8 MeV; C = 5×10^{-4} counts/(keV kg year), $\Delta E = 1\%$ at 2.8 MeV. A half-life of about 2×10^{26} years corresponds to a neutrino mass sensitivity of about 50 meV using matrix elements from Ref. [8].

in Fig. 1. Possible background sources include cosmic rays, the natural radioactive decay chains, radioisotopes produced by cosmic ray interactions within the materials used, and neutrons. To get a first glimpse of the background using CZT detectors, a prototype setup has been installed in the Gran Sasso Underground Laboratory (LNGS) in Italy, which provides an average shielding of ∼3500 mwe against cosmic ray sources.

III. EXPERIMENTAL SETUP

The data presented here were obtained with four $1\times1\times1$ cm^3 CZT semiconductor detectors, each of mass ∼6.5 g, provided by eV-PRODUCTS. They utilize coplanar grid technology to ensure that only the electron signal is read out [9] and hence symmetric energy peaks are obtained. All four crystals were operated at a voltage of −1500 V with a 20- to 40-V grid bias applied between the two anodes. The crystal surfaces, except for the gold-coated cathode side, are covered with a passivation paint that prevents oxidation and deterioration in detector performance over time.

The four detectors were mounted in a copper brick separated from all preamplifier electronics by ∼25 cm. The copper brick was part of a (20 cm)^3 cube of electropolished copper that was embedded in a further 15 cm of lead. The whole setup was located in a Faraday cage made from copper plates. The cage was surrounded by a neutron shield, consisting of 7-cm-thick boron-loaded polyethylene plates and an additional 20 cm of paraffin wax at the bottom. This neutron shield was upgraded to cover three sides of the cage, as well as the base, with paraffin wax before the third data taking period (period C). Data collection commenced with a CAMAC-based data acquisition (DAQ) system in which the signals were fed into four peak-sensing ADC modules (LeCroy 3511 and 3512) via custom-built preamplifiers and shaping main amplifiers. Prior to period C, the system was upgraded to a VME-based DAQ with four custom-built, peak sensing, 14-bit ADC channels.

IV. DATA ACQUISITION

The data analyzed in this article can be divided into three periods, separated by upgrades to the experimental configuration that could have affected the background contributions. In period A, the crystals were held in pertinax mounting plates and connected directly to lemo cables. These mounting materials were replaced by cleaner (in the radiopurity sense) delrin holders, whereas the lemo connections were exchanged for copper traces mounted on kapton foils at the start of period B. Before period C the data acquisition hardware was upgraded to the VME system and the paraffin neutron shielding was completed.

During the latter periods not all crystals were fully operational, so only data from crystal 1 were analyzed. In each period, individual runs were limited to 1 h and selection criteria were applied on a run-by-run basis to reject data affected by "bursts" of abnormally high event rates. Subsequent studies have shown two main causes for such bursts: vibrations of the apparatus that cause a piezoelectric effect in the crystals resulting in false event signals, and breakdown effects due to faulty contacts to the crystal electrodes. To reject the affected data, first, the dead time was calculated from the total number of events per hour and the length of the event readout cycle during which new events could be missed. Two hundred and seven runs in which the dead time exceeded 2% (due to large numbers of events with low ADC counts) were rejected. For the remaining runs the distribution of the number of events per hour in the energy range 300–4000 keV was fitted with a Poissonian distribution. Runs with an event rate exceeding the 99% upper limit of the fitted distribution were discarded from the analysis. A further 203 runs were rejected in this way. No other cuts were applied to the data and in total 2.5% of the runs were rejected.

It is possible that each crystal had different background contributions due to intrinsic and surface contaminants (as indicated by the values in Table I). For this reason, data collected with each crystal, and in each period, were considered

TABLE I. Livetimes for data sets prepared above two different energy thresholds (500 and 600 keV), and an indication of the average background level in the 2- to 3-MeV region.

Subset	Livetime (days)		Events/(keV kg day) in 2- to 3-MeV range
	>500 keV	>600 keV	
1A	32.86	150.99	0.57±0.02
2A	0	112.34	0.59±0.03
3A	52.84	52.84	0.38±0.03
4A	62.62	134.64	0.34±0.02
1B	16.03	16.03	0.54±0.07
1C	197.53	197.53	0.56±0.02

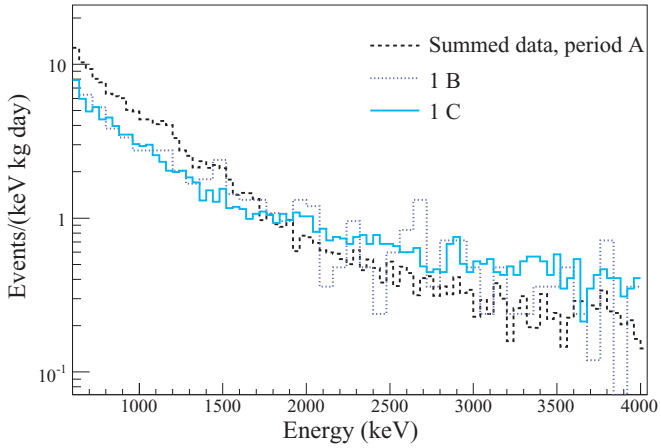

FIG. 2. (Color online) The prepared data sets for periods A, B, and C. Period A comprises data from all four detectors and has slightly less events in the high-energy regions as the background levels in detectors 3 and 4 are lower. However, periods B and C show less events at low energies due to improvements in the cleanliness of mounting materials.

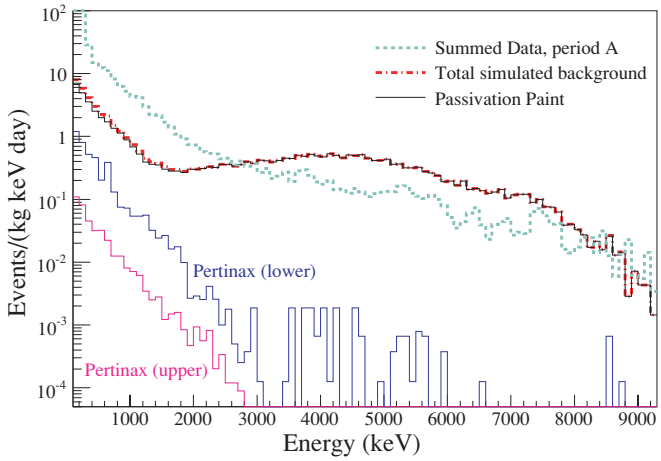

FIG. 3. (Color online) Summed data spectrum for period A, compared to simulated activities of the individual components. This clearly shows that events from the passivation paint on the detector surfaces contribute a significant background to the range of interest (2–3 MeV). The excess of events below 3 MeV is thought to be due to backgrounds associated with the lemo cables and solder.

as a different data subset. The summed data for each of the collecting periods are shown in Fig. 2.

Although detectors have been operated for extensive periods with thresholds below 100 keV, at times it was necessary to raise the threshold for data collection to exclude electronic phenomena. Therefore, to maximize the livetime for analysis, two data sets have been prepared; one with an energy threshold of 600 keV, and one with a 500 keV threshold that omits any runs with thresholds in the range 500–600 keV. The livetimes for each subset and threshold are given in Table I. The total livetime for the high-threshold data set is 4.34 kg·days, whereas the low-threshold data set comprises 2.36 kg·days.

The energy resolution and stability of the detectors was calibrated regularly with the help of ^{137}Cs, ^{60}Co, and ^{228}Th sources. Time-averaged resolution functions were determined for each data subset with all crystals showing a linear increase in full width at half maximum (FWHM) with increasing energy. FWHM values in the range 5–8% at 2809 keV were achieved. Variations in the resolution achieved can be attributed to changes in the contacting methods and the voltages applied between the different data taking periods. It should be noted that the detectors used here do not have the best energy resolution possible, because for this first study with unknown background a very good energy resolution was not considered to be essential and, hence, cheaper detectors were used.

V. BACKGROUND STUDIES

To understand the observed spectrum and disentangle the individual contributions, a background model has been developed. All materials used were measured for contaminants in the LNGS Ge-detector facility, though some of them could only be measured after the start of data taking with the prototype. As a consequence of these measurements, the pertinax holders and lemo cables were replaced by delrin holders and kapton foils (between periods A and B). No contamination of the CdZnTe could be detected with the Ge facility. With the known activities of contaminants in the individual components, extensive Monte Carlo modeling based on GEANT4 was performed to describe the observed spectrum (Fig. 3).

By far the largest background in the 2- to 3-MeV region evolves from the passivation paint on the detector surface. The precise prediction of this contribution varies slightly due to the unknown paint mass and the inhomogeneous paint thickness, which affects the α-particle simulation in particular. However, there is a slight advantage associated with the contaminated paint as the detector effectively acts as a self-calibrating device. The installation of the VME system at the start of period C significantly improved the timing resolution achieved for event read-out (from $\approx$1 ms to $\leqslant$10 μs) permitting the observation of $\beta - \alpha$ coincidence events from ^{214}Bi. This isotope originates from the Th-decay chain, present in the passivation paint, and β decays with an end point of 3.3 MeV; the daughter isotope, ^{214}Po, α decays with a half-life of 164.3 μs, releasing a 7.7 MeV α. The rate of event pairs observed in the period C data set was consistent with the measured activity of a paint sample. Furthermore, it shows that any possible dead layer at the detector surface is insignificant, otherwise the α particles would not be detected. In the meantime, an alternative solution for surface passivation of the CZT detectors has been found and is currently being explored at LNGS. Initial measurements show a reduction of this background by at least a factor of 8, if not more, in the region of interest around 2.8 MeV.

The measurements of pertinax contaminants prompted the replacement of all pertinax components with delrin, leading to a reduction of events by about a factor of 5 in the range 500–2000 keV, though some of this reduction can be attributed to the exchange of the lemo cables.

VI. ACHIEVABLE ENERGY RESOLUTION

The underground studies are not currently limited by energy resolution and, therefore, it was not considered necessary to use the highest quality of crystals in this setup. However, as background levels are reduced the energy resolution will become important, because a sharp peak is especially important in reducing the contribution of the irreducible background of $2\nu\beta\beta$ events to the $0\nu\beta\beta$ peak region. The fraction of $2\nu\beta\beta$ events in the peak region, as a function of energy resolution (FWHM), can be approximated by [10]

$$F = \frac{8Q}{m_e}\left(\frac{\Delta E}{Q}\right)^6. \quad (1)$$

With this in mind, additional studies were performed outside the underground experiment to determine the resolution achievable with CZT coplanar-grid detectors and to investigate possible improvements.

Figure 4 shows a ^{228}Th spectrum measured with a typical "medium quality" CZT detector, resulting in a resolution of 2.6% at 2614 keV but resolutions as good as 2.1% have been measured with COBRA crystals. With such a resolution, for the case of 90% ^{116}Cd isotopic enrichment, $2\nu\beta\beta$ decays will contribute only 2×10^{-4} counts/(kg yr) to the 59-keV wide signal region (calculated using the observed half-life of 2.7×10^{19} yr [11]). This is already well below the required background levels shown in Fig. 1 but detectors with still better energy resolution are commercially available and are being considered for use in a future stage of the experiment.

A further experimental option to improve the energy resolution is cooling of the detector. This might be especially important for searches in the low-energy range, for decays such as two neutrino double electron capture (2νECEC) that produce a signal below 100 keV. First measurements of cooling from 24°C to 10°C revealed an improvement in energy resolution of a factor two below 100 keV and an improvement of 5% on the typical resolution at 2809 keV.

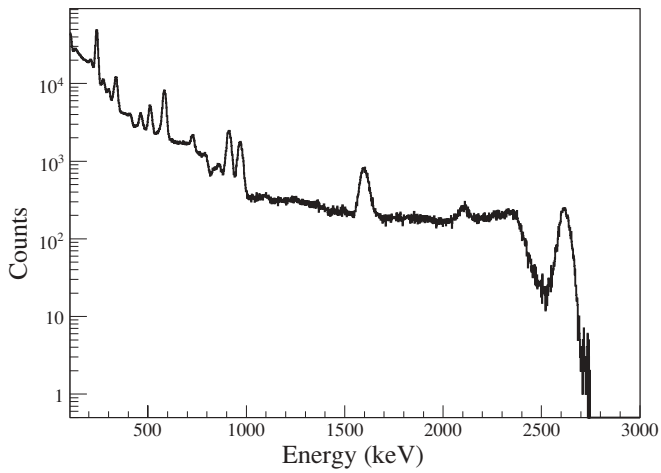

FIG. 4. Energy spectrum of a ^{228}Th calibration source obtained with a 1-cm^3 CZT detector at room temperature of around 24°C. The energy resolution (FWHM) at the 2614-keV line is 2.6%.

TABLE II. Specifications of the fits performed for $\beta^-\beta^-$ peaks. Values given for each decay are the peak energy, E_{peak}, the FWHM (ΔE_{peak}) at that peak energy (range for all six data subsets), the efficiency, ϵ, for observing that peak determined from simulations and the energy range over which the fit was performed.

Isotope and decay	E_{peak} (MeV)	ΔE_{peak} (%)	ϵ (%)	Fit range (MeV)
^{116}Cd to g.s.	2.809	4.7–7.6	66.5	2.21–3.20
^{130}Te to g.s.	2.529	4.8–7.8	70.9	2.21–3.20
^{130}Te to 536 keV	1.993	5.0–8.5	61.2	1.70–2.28
^{116}Cd to 1294 keV	1.511	5.4–9.4	74.4	1.20–1.78
^{116}Cd to 1757 keV	1.048	6.0–11.0	60.4	0.90–1.30
^{70}Zn to g.s	1.001	6.1–11.3	93.3	0.60–1.30
^{128}Te to g.s	0.868	6.5–12.2	94.8	0.60–1.30
^{116}Cd to 2027 keV	0.778	6.8–12.9	67.4	0.50–1.20
^{116}Cd to 2112 keV	0.693	7.1–13.8	77.3	0.50–1.00
^{116}Cd to 2225 keV	0.580	7.7–15.4	76.6	0.50–1.00

VII. DATA ANALYSIS

The data analysis consists of two independent parts: simulation of the possible double β decays to determine detection efficiencies and a maximum likelihood peak search.

The predicted signals in the crystals were determined through a GEANT4-based Monte Carlo simulation utilizing calculations from the Fortran DECAY0 code [12]. $0\nu\beta\beta$ decays to ground state (g.s.) and excited states[1] were simulated for each of the candidate isotopes contained in natural CdZnTe. For $\beta^-\beta^-$ transitions, calculations based on the light Majorana neutrino exchange mechanism were used for $(0^+ \rightarrow 0^+)$ transitions, whereas right-handed currents were used in the calculation for $(0^+ \rightarrow 2^+)$ transitions. As there is no general connection between ground state and excited state matrix elements, they must be explored separately for each isotope.

The energy, E_{peak}, and intensity of the dominant peak for each $\beta^-\beta^-$ decay were determined from these simulations and are given in Table II. The efficiency for observation of the full peak energy, ϵ, determined from the peak intensity generally decreases with increasing peak energy. For decays to excited states, γ escape probabilities also play a part.

For the isotopes that decay through $\beta^+\beta^+$ transitions, double electron capture (EC/EC), single electron capture (β^+EC) and double positron ($2\beta^+$) transitions were considered when energetically possible. In general the predicted spectra for these decays are significantly more complex than those for $\beta^-\beta^-$ transitions, without clearly dominating peaks. As an example, the simulated spectrum for ^{64}Zn β^+EC decays to the ground state is shown in Fig. 5, both for ideal resolution and convolved with the energy response for data subset 1A. Although there is a peak at the Q value for this decay (1096 keV), there are also single and double 511-keV escape peaks, and a peak at 511 keV due to γs produced from the

[1]Only excited states already included in the DECAY0 code were used, therefore some transitions, namely those to the higher excited states of ^{120}Te, have been omitted from this analysis.

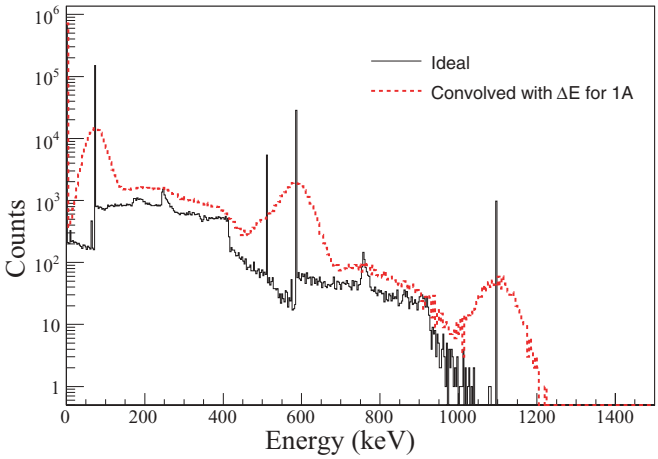

FIG. 5. (Color online) Simulated spectrum in crystal 1 for ^{64}Zn β^+EC decays to the ground state for ideal resolution and convolved with the energy response for data subset 1A.

annihilation of positrons produced by these decays in the other three crystals.

Detailed simulations and ex situ measurements of background contaminants were used to characterize the measured background continuum, as described in Sec. V. An exponential of the form $y = A + Be^{-Cx}$ was found to describe the data well at higher energies. Below 500 keV the fits were less satisfactory due to the presence of a number of low-energy γ peaks and the fourfold forbidden decay of ^{113}Cd [13] so a 500-keV threshold was enforced. Thus, decay modes with no significant peaks above 500 keV, namely those of ^{108}Cd and ^{114}Cd, were omitted from the analysis presented in this article.

A study of the residuals of the background fits showed some evidence for additional peaks in the continuum at 609 and 1120 keV, relating to γ lines from ^{214}Bi decay. Due to the combined effects of decay branching ratios, energy resolution and reduced efficiency for stopping higher energy γs in a single crystal, no other background γ peaks within the analysis region were predicted through simulations. Therefore, two Gaussian peaks were added to the description of the background with fixed mean and width determined from the relevant resolution function. The amplitudes of these peaks were treated as additional fit parameters. As a cross-check, fits for the exponential background were performed without these additional background peaks and in all cases resulted in a poorer, or negligibly different, chi-squared probability.

A maximum likelihood fit was performed to determine the most likely number of signal events, θ_s, over the combined data set. Parameters describing the background were allowed to vary between crystals and data collection periods, but the $0\nu\beta\beta$ signal rate was assumed to be constant throughout. That is, different background parameters were applied to different data subsets to allow for the varying background rates (indicated in Table I) but the normalized background distributions fitted to each data subset were found to agree within errors for each fit scenario.

For $\beta^-\beta^-$ modes, θ_s enters the fit through the amplitude of a Gaussian peak with width determined by the calibrated resolution of the relevant data subset. The range of peak widths (FWHM) for each fitted peak are given in Table II along with the energy range used for each fit. Simulations showed that a range of $(E_{\text{peak}} \pm 3\Delta E)$ or greater was required for each peak search to adequately characterize the background continuum. The close proximity of some predicted signal peaks required these ground-state transition signals to be determined simultaneously: ^{116}Cd and ^{130}Te were fit together and the ^{70}Zn and ^{128}Te peaks were also fit simultaneously. Transitions to excited states are expected to be significantly suppressed with respect to ground-state transitions due to phase-space arguments, so any contribution of excited state decays to the fitted peaks for ground-state transitions is assumed to be negligible. The limit for each signal arising from a transition to an excited state was determined in a separate fit. The high-threshold (>600 keV) data set was used for all $\beta^-\beta^-$-mode peak searches except the decays to the third and fourth excited states of ^{116}Cd.

The majority of spectra predicted for $\beta^+\beta^+$-mode decays have multiple peaks, each significantly smaller in amplitude than those arising from $\beta^-\beta^-$ decays to the ground state, thus justifying separate treatment in the analysis. Due to the complexity of these spectra, to determine the most likely number of signal events, θ_s, the most likely scaling factor

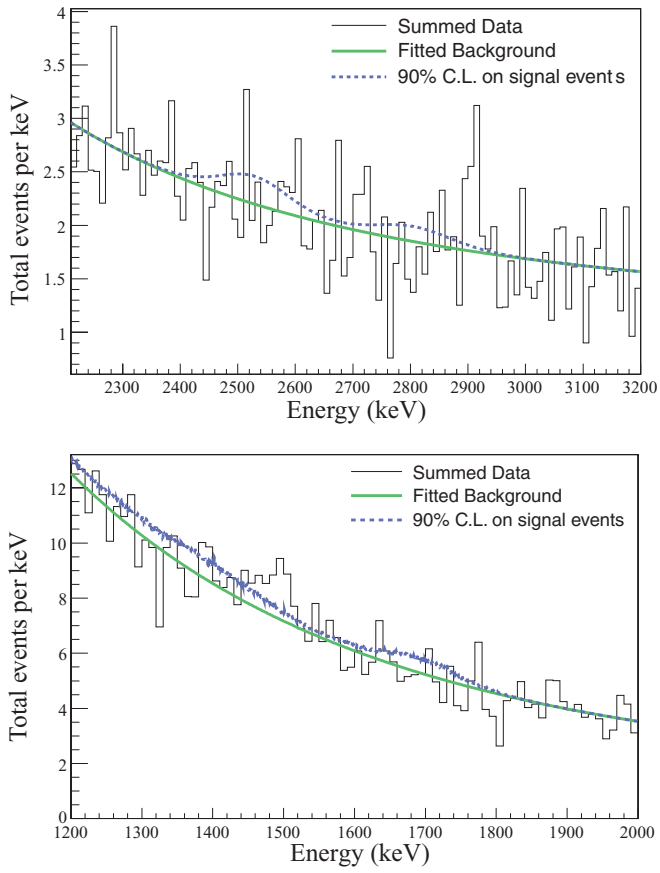

FIG. 6. (Color online) The fitted 90% confidence limits for ^{116}Cd and ^{130}Te $0\nu\beta\beta$ decay events (top) and ^{120}Te 0νEC/EC to ground state events (bottom) with the total high-threshold data set shown for the range of each fit. Also shown separately is the contribution from the fitted background.

TABLE III. Results from fits for $\beta^-\beta^-$ decay peaks. The χ^2/DOF goodness-of-fit parameter, and respective probability determined through Monte Carlo are included. The 90% confidence limits have conservative systematic uncertainties applied and are compared to the world best limits.

Isotope and decay	χ^2/DOF	P	$T_{1/2}$ limit (years)	
			This work	World best
^{116}Cd to g.s.	1236/2950	0.99	3.14×10^{19}	1.7×10^{23} [14]
^{130}Te to g.s.	1236/2950	0.99	9.92×10^{19}	1.8×10^{24} [15]
^{130}Te to 536 keV	726/1703	0.99	3.73×10^{19}	9.7×10^{22} [16]
^{116}Cd to 1294 keV	676/1703	1.00	4.92×10^{18}	2.9×10^{22} [14]
^{116}Cd to 1757 keV	615/1479	0.99	9.13×10^{18}	1.4×10^{22} [14]
^{70}Zn to g.s.	859/2078	1.00	2.24×10^{17}	9.0×10^{17} [17]
^{128}Te to g.s.	859/2078	1.00	5.38×10^{19}	1.1×10^{23} [18]
^{116}Cd to 2027 keV	756/1732	0.96	1.37×10^{19}	2.1×10^{21} [19]
^{116}Cd to 2112 keV	545/1233	0.87	1.08×10^{19}	6.0×10^{21} [14]
^{116}Cd to 2225 keV	545/1233	0.87	9.46×10^{18}	1.0×10^{20}[a] [20]

[a]Quoted limit is 68% not 90%.

for the entire simulated spectrum, was extracted from the likelihood fit. For each decay the simulated spectrum was normalized to unity and convolved with the relevant resolution function for each data subset. The range for each fit (as given in Table IV) was selected to include all the dominant peaks. For transitions where the simulated spectra showed a dominant peak in the region 500–600 keV, the low-threshold data set was used; in all other cases, the high-threshold data set was used.

For all $\beta^-\beta^-$ and $\beta^+\beta^+$ modes analyzed, a 90% confidence limit on the half-life, T_{half}, was determined from the fitted number of signal events, $\theta_s \pm \delta_s$, where δ_s is one sigma uncertainty in the fit, for each decay under investigation.

$$T_{\text{half}} = \frac{N_{\text{iso}} t_{\text{live}} \epsilon \ln 2}{(\theta_s + 1.28\delta_s)}. \tag{2}$$

Here N_{iso} is the number of candidate nuclei per crystal for the given decay, t_{live} is the total duration of data collection in crystal-years, and ϵ is an efficiency factor determined from simulations. For $\beta^-\beta^-$-searches, ϵ is the fraction of simulated events in the peak region (see Table II). However, for $\beta^+\beta^+$-searches $\epsilon = 1$ because the whole simulated spectrum, normalized to unity, is used in the fit.

For each fit, a chi-squared goodness of fit test was performed. However, due to the low statistics, this parameter was not expected to follow a true chi-squared distribution. Therefore, the distribution of the χ^2 statistic was determined by Monte Carlo for each fit to calculate the fit probability. The χ^2, and its respective probability, determined for each $\beta^-\beta^-$ fit is included in Table III. For the $\beta^+\beta^+$ fits the probabilities for each fit were also all >80%. As a cross-check, fits were repeated with θ_s fixed to zero for each signal, all of which resulted in either negligible change or a decrease in the goodness of fit.

A detailed study of possible systematic effects was performed and the dominant uncertainties were found to be those that affect the number of candidate nuclei. Uncertainties in

TABLE IV. 90% confidence limits obtained for all $\beta^+\beta^+$ decays analyzed in this work with conservative systematic uncertainties applied, compared to the world best limits. New world best values from this work are shown in bold. The energy range used for each fit is also included.

Isotope and decay	Range (MeV)	$T_{1/2}$ limit (years)	
		This work	World best
^{64}Zn $0\nu\beta^+$EC to g.s.	0.5–1.3	2.78×10^{17}	2.4×10^{18} [17]
^{64}Zn 0ν2EC to g.s.	0.7–1.3	1.19×10^{17}	7.0×10^{16} [17]
^{120}Te $0\nu\beta^+$EC to g.s.	0.5–2.0	1.21×10^{17}	2.2×10^{16} [21]
^{120}Te 0ν2EC to g.s.	1.2–2.0	2.68×10^{15}	–
^{120}Te 0ν2EC to 1171 keV	0.5–2.0	9.72×10^{15}	–
^{106}Cd $0\nu\beta^+\beta^+$ to g.s.	0.5–2.0	4.50×10^{17}	2.4×10^{20} [22]
^{106}Cd $0\nu\beta^+$EC to g.s.	1.4–3.0	7.31×10^{18}	3.7×10^{20} [22]
^{106}Cd 0ν2EC to g.s.	1.4–3.0	5.70×10^{16}	1.5×10^{17} [23]
^{106}Cd $0\nu\beta^+\beta^+$ to 512 keV	0.5–2.0	1.81×10^{17}	1.6×10^{20} [22]
^{106}Cd $0\nu\beta^+$EC to 512 keV	0.8–2.0	9.86×10^{17}	2.6×10^{20} [22]

energy resolution and livetime, and possible biases in the fit procedure, were all found to have a negligible effect on the analysis. However, the possible existence of a dead-layer at the surface of the crystals could reduce the active volume by up to 10%. Observations of α-particles from the passivation paint indicate that the dead layer is probably smaller than this but the effect was taken into account in a conservative manner by using $N_{\mathrm{iso}} \times 0.9$ in the limit calculation. Due to the production process, the zinc content is known to be only in the range 7–11%, resulting in an uncertainty in both the number of zinc nuclei and the number of cadmium nuclei. To ensure conservative half-life limits, 7% zinc content was used when calculating the number of zinc nuclei, and 11% zinc content was used in calculations for cadmium isotopes.

VIII. RESULTS

Table III shows all the $\beta^-\beta^-$-decay half-life limits (90% C.L.) calculated in this work and Table IV shows the limits calculated for $\beta^+\beta^+$-decays. The limits obtained from the combined fit to the ^{116}Cd and ^{130}Te $0\nu\beta\beta$ decays to ground state and for the ^{120}Te double electron capture decay to ground state are shown in Fig. 6. Due to the small detector mass, at present the searches for ^{116}Cd and ^{130}Te cannot compete with other running large scale experiments. However, half-life limits obtained for ^{64}Zn and ^{120}Te improve on existing measurements.

IX. SUMMARY

A new double β-decay experiment, COBRA, is planned using a large amount of CZT semiconductor detectors. A low rate of background events in the peak region and good energy resolution are crucial aspects of the design of such an experiment. To develop this new approach, CZT semiconductor detectors were operated deep underground, for the first time, to study their background. Using a small prototype, a background model was developed and a major background component in the form of a passivation paint on the detector surfaces was identified. Alternatives are now available and major improvements are expected soon.

Studies of the attainable energy resolution showed that the contribution of the irreducible background of $2\nu\beta\beta$ can be kept to a negligible level. A 4.34 kg·day data set, collected with four 1-cm^3 crystals, was analyzed to determine limits on various neutrinoless double β decay modes of seven different isotopes. Despite the small detector mass, only 26 g of CZT, these data have yielded four improved half-life limits for decays of ^{64}Zn and ^{120}Te. After submission of this article new limits for ^{120}Te were presented [24].

In the near future, 64 CZT detectors will be running and improvements on all the limits presented in this article can be expected. In addition to the increased detector mass, new criteria based on coincident energy deposits in time and space will allow better rejection of backgrounds, and a full characterization of each individual crystal will help reduce systematic uncertainties.

ACKNOWLEDGMENTS

We thank G. Cowan for useful discussions, V. Tretyak for providing the DECAY0 code, and eV-PRODUCTS for their support. In addition, we thank the Forschungszentrum Karlsruhe, especially K. Eitel, for providing the material for the neutron shield. We thank the mechanical workshop of the University Dortmund for their support and the Laboratori Nazionali del Gran Sasso (LNGS) for offering the possibility to perform measurements underground. This research was supported by PPARC and the Deutsche Forschungsgemeinschaft (DFG). The work has been supported by the TA-DUSL activity of the ILIAS program (contract RII3-CT-2004-506222) as part of the EU FP6 programme.

[1] Y. Fukuda *et al.*, Super-Kamiokande Collaboration, Phys. Rev. Lett. **81**, 1562 (1998); **82**, 1810 (1999); **82**, 2430 (1999); **86**, 5651 (2001).
[2] Q. Ahmad *et al.*, SNO Collaboration, Phys. Rev. Lett. **87**, 071301 (2001); **89**, 011301 (2002); **89**, 011302 (2002).
[3] K. Eguchi *et al.*, KamLAND Collaboration, Phys. Rev. Lett. **90**, 021802 (2003); **94**, 081801 (2005).
[4] K. Zuber, Acta Phys. Pol. B **37**, 1905 (2006).
[5] S. Elliott and J. Engel, J. Phys. G **30**, R183 (2004).
[6] K. Zuber, Phys. Lett. **B519**, 1 (2001).
[7] M. Hirsch, K. Muto, T. Oda, and H. Klapdor-Kleingrothaus, Z. Phys. A **347**, 151 (1994).
[8] V. Rodin *et al.*, Nucl. Phys. **A766**, 107 (2006).
[9] P. Luke, IEEE Trans. Nucl. Sci. **42**, 207 (1995).
[10] S. Elliott and P. Vogel, Annu. Rev. Nucl. Part. Sci. **52**, 115 (2002).
[11] R. Saakyan, "Results from NEMO III and future plans for SuperNEMO" (2006), DBD06-ILIAS/N6 WGI Collaboration meeting, Valencia, http://ahep.uv.es/dbd06.
[12] O. A. Ponkratenko, V. Tretyak, and Y. Zdesenko, Phys. Atom. Nucl. **63**, 1282 (2000). The actual generator used was DECAY0, not DECAY4.
[13] C. Goessling, M. Junker, H. Kiel, D. Muenstermann, S. Oehl, and K. Zuber, Phys. Rev. C **72**, 064328 (2005).
[14] F. A. Danevich *et al.*, Phys. Rev. C **68**, 035501 (2003).
[15] C. Arnaboldi *et al.*, Phys. Rev. Lett. **95**, 142501 (2005).
[16] A. Alessandrello *et al.*, Phys. Lett. **B486**, 13 (2000).
[17] F. A. Danevich *et al.*, Nucl. Instrum. Methods A **544**, 553 (2005).
[18] C. Arnaboldi *et al.*, Phys. Lett. **B557**, 167 (2003).
[19] A. Piepke *et al.*, Nucl. Phys. **A577**, 493 (1994).
[20] A. Barabash, A. Kopylov, and V. Cherehovsky, Phys. Lett. **B249**, 186 (1990).
[21] H. Kiel, D. Münstermann, and K. Zuber, Nucl. Phys. **A723**, 499 (2003).
[22] P. Belli *et al.*, Astropart. Phys. **10**, 115 (1999).
[23] E. Norman and M. DeFaccio, Phys. Lett. **B148**, 31 (1984).
[24] A. Barabash *et al.*, nucl-ex/0703020 (2007).